Reference: T.W.Petrie, J.A. Atchley, P.W. Childs and A.O. Desjarlais. "Effect of Solar Radiation Control on Energy Costs – A Radiation Control Fact Sheet for Low-Slope Roofs," *Proceedings on CD, Performance of the Exterior Envelopes of Whole Buildings VIII: Integration of Building Envelopes*. December 2001. Paper 146. Atlanta, GA: American Society of Heating, Refrigerating and Air-Conditioning Engineeers, Inc.

Effect of Solar Radiation Control on Energy Costs – A Radiation Control Fact Sheet for Low-Slope Roofs (with post-publication corrections to Table 4 and Figure 4)

by

Thomas W. Petrie, Jerald A. Atchley, Phillip W. Childs and André O. Desjarlais
Buildings Technology Center
Oak Ridge National Laboratory

Prepared by the
Buildings Technology Center
Oak Ridge National Laboratory
Oak Ridge, Tennessee 37831

managed by
UT-Battelle, LLC
for the U.S. Department of Energy
under contract No. DE-AC05-00OR22725

Effect of Solar Radiation Control on Energy Costs – A Radiation Control Fact Sheet for Low-Slope Roofs

Thomas W. Petrie, Ph.D. Member ASHRAE Jerald A. Atchley Phillip W. Childs André O. Desjarlais

Abstract

Low-slope roofs on commercial buildings are exposed to the full amount of horizontal solar radiation. The solar radiation that is absorbed heats the roof surface. The absorbed solar energy, now characterized by the roof surface temperature, is partially reemitted in the infrared spectrum. By selecting or coating a low-slope roof so it has a medium to high solar reflectance and a low to high infrared emittance, the desired amount of solar radiation control is achieved. In this paper, background is presented on the development of an interactive estimating tool to assist commercial building owners and/or operators in selection of a roof. If the low-slope roof is given solar radiation control, the estimating tool indicates the annual savings in operating costs to condition a building under the roof. Alternatively, the tool can give the amount of conventional thermal insulation without radiation control that a roof needs in order to have the same annual energy costs as the roof with the existing amount of conventional insulation and solar radiation control. The tool is part of a fact sheet on solar radiation control for low-slope roofs. The fact sheet is on our Internet web site.

Keywords

commercial building; energy estimating; heat gain; heat loss; insulation; operating cost; solar radiation; low-slope roof

Effect of Solar Radiation Control on Energy Costs – A Radiation Control Fact Sheet for Low-Slope Roofs

Thomas W. Petrie, Ph.D.[1] Jerald A. Atchley Phillip W. Childs André O. Desjarlais
Member ASHRAE

ABSTRACT

Low-slope roofs on commercial buildings are exposed to the full amount of horizontal solar radiation. The solar radiation that is absorbed heats the roof surface. The absorbed solar energy, now characterized by the roof surface temperature, is partially reemitted in the infrared spectrum. By selecting or coating a low-slope roof so it has a medium to high solar reflectance and a low to high infrared emittance, the desired amount of solar radiation control is achieved. In this paper, background is presented on the development of an interactive estimating tool to assist commercial building owners and/or operators in selection of a roof. If the low-slope roof is given solar radiation control, the estimating tool indicates the annual savings in operating costs to condition a building under the roof. Alternatively, the tool can give the amount of conventional thermal insulation without radiation control that a roof needs in order to have the same annual energy costs as the roof with the existing amount of conventional insulation and solar radiation control. The tool is part of a fact sheet on solar radiation control for low-slope roofs. The fact sheet is on our Internet web site.

INTRODUCTION

In June 1997, the Buildings Technology Center at the Oak Ridge National Laboratory began a three-year program of research under the auspices of User Agreements with the Roof Coating Manufacturers Association (RCMA) and several member companies. The goal was to measure and model the thermal performance of the range of low-slope roof coatings under weathering conditions imposed by the East Tennessee climate. Ultimately, the work sought to generalize the results of the tests in East Tennessee by determining how much energy could be saved by coatings in the variety of U.S. climates, from cooling-dominated to heating-dominated.

At the end of the three-year period of performance of the RCMA project, we extended the work slightly by undertaking to clean the test roofs with commercially available cleaning solutions. The solar reflectances of the roofs, which had gradually decreased for all surfaces except one due to the effects of weathering, increased significantly for most surfaces. This made more difficult the desired generalization of thermal performance.

Solar reflectance and infrared emittance are known to be the principal surface properties that affect the thermal performance of roof coatings (Akbari and Konopacki 1999, Wilkes et al. 2000). In the RCMA project, we found that the kind of coating and its history yielded a wide range of solar reflectance and infrared emittance values. We studied white latex coatings, aluminum coatings and special coatings, including an

[1]T.W. Petrie is a research engineer, J.A. Atchley is a research technician, P.W. Childs is a staff engineer, and A.O. Desjarlais is a program leader in the Buildings Technology Center, Oak Ridge National Laboratory, Oak Ridge, Tennessee, U.S.A.

aluminized asphalt emulsion and thin-metal capsheets factory-adhered to low-slope roof membranes.

To achieve the generalization of thermal performance that the project required, we decided to publish a solar radiation control fact sheet on our Internet web site. This fact sheet includes an estimating tool to predict the heating and cooling loads per unit area of a low-slope roof. The user of the estimator specifies surface radiation properties, insulation level and location for the roof. The fact sheet presents the range of radiation properties that resulted from the tests and other information to guide the user of the tool in applying it to conditions of interest. The user then enters local energy costs and average equipment efficiencies to generate annual operating cost savings due to the proposed surface radiation properties and insulation level.

Data from the RCMA project for specific values of fully-weathered roof surface properties, insulation levels and location have already been presented (Wilkes et al 2000). This paper adds data on the effect of cleaning on surface properties and further validates the roof model used to generalize the test results. The main focus, however, is to document the development of the estimating tool. The full range of U.S. climates is available to the tool and the fitting equations used in it permit input of the full range of expected solar reflectance, infrared emittance and thermal insulation level for low-slope roofs. In this paper, net annual cost savings due to radiation control with the scheme implemented in the estimator are compared to predictions for whole buildings with the building annual energy use program DOE 2.1 (LBNL 1993). To illustrate results, the estimator is exercised to give annual energy savings and operating cost savings with radiation control in several locations over the range of roof configurations. Also illustrated is the amount of additional insulation without radiation control that the energy savings with radiation control justify. Some early results are given from the ongoing extension of the scope of work to include peak power savings due to radiation control.

RADIATION PROPERTIES OF LOW-SLOPE ROOF SURFACES

Low-slope roofs on commercial buildings are exposed to the full amount of horizontal solar radiation. The solar reflectance of the surface gives the fraction of incident solar radiation that is reflected. Since the surfaces are opaque to thermal radiation, the solar radiation that is not reflected is absorbed. The solar radiation that is absorbed heats the roof surface. The absorbed solar energy, now characterized by the roof surface temperature, is partially reemitted in the infrared spectrum. The infrared emittance of the surface gives the fraction of the maximum possible infrared radiation that the surface reemits. By selecting or coating a low-slope roof so it has a medium to high solar reflectance and a low to high infrared emittance, the desired amount of solar radiation control is achieved relative to an uncoated surface. Asphaltic materials typically used for low-slope roof membranes without solar radiation control have very low solar reflectance but high infrared emittance.

The degradation of the solar reflectance of surfaces exposed to the weather is well-documented (Byerley and Christian 1994; Bretz and Akbari 1997; Petrie et al. 1998; Wilkes et al. 2000). The emphasis in the work by Byerley and Christian, Bretz and Akbari and Petrie et al. was on white latex coatings because of their very high initial solar reflectance and high infrared emittance. These properties make them good candidates for solar radiation control in cooling-dominated climates. Wilkes et al. show results from the

RCMA project, which also included study of aluminum coatings and a few special coatings. The special coatings were an aluminized asphalt emulsion and two capsheets. The capsheets were aluminum sheets that were factory adhered to low-slope roof membrane material which, in turn, were applied to roof membranes in the field. One capsheet exposed bare aluminum and the other was factory finished with a white coating.

This paper updates the solar reflectances and infrared emittances presented in Wilkes et al. and extends them to show the effect of cleaning on the variety of low-slope roof surfaces. Figure 1 presents the history of solar reflectances measured from June 1997 through October 2000 for 27 different surfaces. The capsheet with a white factory finish is not included. It behaved like an average white latex coating. Different symbols are used for eight white latex coatings, 13 aluminum coatings, four uncoated surfaces, the bare aluminum capsheet and the aluminized asphalt emulsion. Solar reflectances were measured with a portable solar reflectometer at regular intervals from spring through fall, monthly in the first summer of the project. Each data point shown is the average of measurements at four uniformly appearing locations on the 0.61 m (2 ft) square test sections. The measurement head opening of the reflectometer covers a 2.5 cm (1 in.) diameter circular area of test surface during a measurement.

The legend of Figure 1 indicates the time at which all the test roofs were cleaned by gently scrubbing them with a solution of trisodium phosphate (TSP) in water and thoroughly rinsing them. TSP attacked the organic growths and dirt on both aluminum-coated and white latex-coated surfaces without harming either type of coating. The behavior of the solar reflectances also shows clearly when cleaning was done. With the exceptions of the uncoated surfaces, the aluminum-coated surface with the lowest reflectance and the aluminized asphalt emulsion, solar reflectances increased significantly due to cleaning. Surfaces whose solar reflectances increased appeared brighter after cleaning. The solar reflectances of the uncoated surfaces and the lowest reflectance aluminum were not affected by the cleaning. The aluminized asphalt emulsion surface noticeably darkened although its solar reflectance recovered somewhat in the subsequent months. It is speculated that cleaning of this surface exposed the asphalt emulsion, which aluminum particles had gradually masked as this surface weathered.

The solar reflectances of the white latex and aluminum coatings displayed an average increase of 0.11 relative to pre-cleaning values. The white latex coatings before cleaning had reflectances that were, on average, 0.27 lower than fresh values. Thus, cleaning restored about 41% of the decrease due to weathering. The aluminum coatings before cleaning had reflectances that were, on average, 0.20 lower than fresh values. Thus, cleaning restored about 55% of the decrease due to weathering. The effect of cleaning persisted for the few months available for observation until the test roofs were dismantled for post-project analysis by RCMA.

Second-order polynomials are shown through the data for the uncoated surfaces, the white latex-coated surfaces with the highest and lowest reflectance, the aluminum-coated surfaces with the highest and lowest reflectance, the bare aluminum capsheet and the aluminized asphalt emulsion. They are from least-squares regressions for each surface of the reflectances with time from the beginning of the project until just before the surfaces were cleaned. The initial solar reflectance for the aluminum coatings was ignored in the regressions because aluminum coatings typically require a few weeks to cure after being applied. The white latex-coated and aluminum-coated surfaces with the

highest and lowest reflectances were selected based on performance after two years and two months of weathering. The aluminum with the highest reflectance at two years and two months was not the aluminum with the highest reflectance during the first summer of the project. Only the solar reflectance curve for the white latex coating with the highest reflectance continued to decrease after two years and two months of weathering until the time of cleaning. The minimum that is shown by several curves is an artifact of the second order polynomial that was selected as the fitting function. Our judgment is that the surfaces were fully weathered by two years and two months (780 days) into the project.

Fully-weathered solar reflectances and infrared emittances for the various surfaces are summarized in Table 1. To aid in judgments about appropriate thermal radiation properties for typical coated surfaces, values for the average white latex coating and average aluminum coating are included in the table. The solar reflectance values are obtained from the least squares regressions evaluated at two years and two months. The surfaces used for the averages do not include the ones that displayed the highest or lowest reflectances. The uncertainty in the values of solar reflectance is ±0.02 (Wilkes et al. 2000).

Measurements of infrared emittance were made annually during the RCMA project with a portable emissometer. They showed no effects of weathering after the first year of the project within the uncertainty of ±0.05 in the readings (Childs et al. 2001). Cleaning did not affect the infrared emittances of the uncoated or white latex-coated surfaces but lowered the average infrared emittance of the aluminum-coated surfaces by about 0.15.

TABLE 1.
Fully-Weathered Solar Reflectances and Infrared Emittances of
Uncoated and Coated Low-Slope Roof Surfaces

Surface[2]	Solar Reflectance	Infrared Emittance
Highest Reflectance White Latex Coating	0.68	0.90
Average White Latex Coating	0.55	0.90
Lowest Reflectance White Latex Coating	0.47	0.82
Highest Reflectance Aluminum Coating	0.49	0.52
Average Aluminum Coating	0.38	0.57
Lowest Reflectance Aluminum Coating	0.24	0.68
Aluminized Asphalt Emulsion Coating	0.34	0.90
Bare Aluminum Capsheet	0.66	0.11
Uncoated Surface	0.05	0.90

[2] Highest, average and lowest reflectance refer to values for white latex and aluminum coatings observed after two years and two months of weathering.

MODELING THERMAL PERFORMANCE OF LOW-SLOPE ROOFS

Low-slope roofs on commercial or industrial buildings are simple structures. Away from the roof edge or penetrations, heat transfer is one-dimensional. The layers that comprise the roof are typically a deck for structural support, insulation for acceptable thermal performance and a membrane for waterproofing. In this work we are also interested in using the outside surface of the membrane for solar radiation control. The layers have different thermal properties because of their different materials but heat transfer occurs sequentially through the layers. The heat transfer is very time dependent because it is driven by the ambient weather conditions.

At our laboratory, K.E. Wilkes (Wilkes 1989) developed and validated a model called Simplified Transient Analysis of Roofs (STAR) to predict heat flows and temperatures within low-slope roof systems having known thermal properties. The thermal properties of the various layers comprising the roof may vary with temperature. STAR is fully coupled to ambient weather conditions and can accommodate weather files in compilations such as the Typical Meteorological Year (TMY2) data set (NREL 1995). Alternately, STAR can use weather data that was measured along with the thermal performance of the test roofs in the RCMA project.

The ability of STAR to predict accurately the thermal performance of low-slope roofs over a wide range of surface radiation properties was not comprehensively validated in the development of STAR. Among the measurements we made continuously for all the test roofs in the RCMA project were membrane temperature and heat flux through the wood fiberboard insulation in the roofs. To measure membrane temperature, a thermocouple was placed against the underside of the membrane after it was adhered to the top layer of insulation. To measure insulation heat flux, a thin 5.1 cm (2 in.)-square heat flux transducer was placed between the top 1.25 cm (0.5 in.)-thick layer and bottom 2.5 cm (1.0 in.)-thick layer of wood fiberboard insulation in a depression routed out of the bottom layer.

To validate STAR for the variety of roof surfaces in the RCMA project, several cloudless days throughout the project were selected for detailed modeling of thermal performance. Figure 2 compares measured and predicted membrane temperatures for two white latex-coated surfaces (R53E85 and R48E82), four aluminum-coated surfaces (R34E60, R26E68, R36E64 and R42E56) and two uncoated surfaces (R05E92 and R05E87) in mid-August of 1999, two years and two months into the project. Air temperatures are shown for comparison to the membrane temperatures. Figure 3 compares measured and predicted insulation heat fluxes for the same surfaces and time. Mid-August 1999 is when we judged the surfaces to be fully weathered and is the time at which Table 1 presents typical solar reflectances and infrared emittances. The specific surfaces in Figures 2 and 3 are identified by the code RxxEyy where xx is the percent solar reflectance and yy is the percent infrared emittance for each. Relative to the surfaces in Table 1, the white latex coatings and the aluminum coatings in Figures 2 and 3 have average to below average solar reflectances in the ranges for the respective types.

The measurements shown as solid or dashed curves in Figures 2 and 3 are drawn through 15 minute averages of data acquired every minute. The predictions shown as triangles, squares, circles or diamonds are hourly output values from STAR. Calculations

were done at 15 minute intervals with a fully implicit, stable, finite difference algorithm. As shown by Figures 2 and 3, STAR slightly underpredicts temperatures and heat fluxes relative to the measurements for some surfaces and slightly overpredicts for others. However, many predictions are the same as the corresponding measurements both day and night.

Figures 2 and 3 show the ability of STAR to produce predictions that, like the measurements, clearly differentiate among white latex coatings, aluminum coatings and uncoated surfaces. The white latex-coated surfaces with high solar reflectance and high infrared emittance exhibit the low membrane temperatures and low heat fluxes. The uncoated surfaces with low solar reflectance and high infrared emittance exhibit the high membrane temperatures and high heat fluxes. The aluminum-coated surfaces have solar reflectances between the values for the white latex-coated and uncoated surfaces and have lower infrared emittances than the other surfaces. They exhibit membrane temperatures and heat fluxes that are not as high as those of the uncoated surfaces. Their membrane temperatures and heat fluxes are clearly higher than those of the white latex-coated surfaces. This further substantiates the claim that solar reflectance and infrared emittance are the principal properties of the surfaces affecting thermal performance. Thermal resistance and thermal mass of the whole roof assembly are also important.

Sensitivity analysis for surfaces R42E56 and R36E64 was done with STAR to see the effect of the inherent uncertainties in the measurements of the solar reflectance and infrared emittance. It showed that a ±0.02 change in solar reflectance in STAR caused a ±2°F change in membrane temperature and a ±0.6 Btu/h·ft² change in heat flux at peak conditions. A ±0.05 change in infrared emittance caused a ±2-3°F change in membrane temperature and a ±1.0 Btu/h·ft² change in heat flux at peak conditions. The larger change in infrared emittance needed to cause the same effect on membrane temperature and insulation heat flux means the effect on roof thermal performance of infrared emittance is slightly less strong than that of solar reflectance. At night solar reflectance is not important but a ±0.05 change in infrared emittance caused less than a ±1°F change in membrane temperature and negligible change in heat flux.

The underprediction of peak membrane temperatures relative to the measurements for surface R42E56 and underprediction of peak heat fluxes for surface R36E64 are slightly larger than the sensitivity analysis indicates as the possible effect of uncertainties in solar reflectance and infrared emittance. Our judgment is that the measurements of membrane temperatures and insulation heat fluxes have inherent uncertainty of ±5°F and ±2.0 Btu/h·ft², respectively, at peak conditions. Some unexplained differences between measurements and predictions are to be expected with so many surfaces undergoing simultaneous testing and with both predictions and measurements subject to uncertainties from independent measurements.

Generally, despite the situation for surfaces R42E56 and R36E64, membrane temperatures are slightly overpredicted relative to measurements. Peak heat flux predictions and measurements agree within expected uncertainty. This is consistent with the membrane temperature measurements being made underneath the coating and membrane while membrane temperatures are predicted at the top surface in the model. The heat flux measurements and predictions were both made exactly between the two layers of roof insulation.

STAR is able to predict temperatures and heat fluxes throughout roofs. The effect of the roof on the conditioned space under the roof is of most interest for operating cost savings. For this, the heat flux at the bottom of the roof deck is needed. Wilkes et al. (2000) presented evidence to validate STAR for use with yearly weather files such as TMY2. Hourly deck heat fluxes were predicted by STAR and entered into workbooks of a spreadsheet for a particular location. Each workbook corresponded to a specific set of roof surface radiation properties, roof insulation level and deck construction.

Two new columns were generated in each workbook. In one, deck heat fluxes into the conditioned space were copied for each hour of the year when the outside air temperature was greater than 24°C (75°F). Otherwise, nothing was entered. The sum of these heat fluxes is defined as the annual cooling load per unit area of roof, CL. In the other column, deck heat fluxes out of the conditioned space were copied for each hour of the year when outside air temperature was less than 16°C (60°F). Otherwise, nothing was entered. The sum of these heat fluxes is defined as the annual heating load per unit area of roof, HL. The deadband between cooling and heating was imposed to model the switch over from heating to cooling and vice versa that is done in commercial buildings. The definitions should account for most of the annual heating and cooling load due to the roof.

Wilkes et al. (2000) presented annual cooling and heating loads for various roofs and for various climates. They showed that white latex-coated surfaces permit the most energy savings relative to uncoated surfaces in cooling-dominated climates. The relatively low infrared emittance of the bare aluminum capsheet along with its relatively high solar reflectance caused this surface to display the most energy savings in mixed and heating-dominated climates. They emphasized that conventional insulation is more effective than radiation control for energy saving in heating-dominated climates. Regardless of surface coating, energy savings were economically significant only in cooling-dominated climates with poorly insulated roofs. This finding is often couched in terms of confusing advertising claims about the R-value equivalency of radiation control to conventional insulation in cooling-dominated climates.

DEVELOPMENT OF THE ESTIMATING TOOL

As explained in the previous section, annual heating loads, HL, and cooling loads, CL, per unit area of various low-slope roof configurations were generated by STAR using TMY2 typical meteorological year weather data. Locations were selected to include climates that ranged from cooling-dominated to heating-dominated. Inside temperature below the roofs was held at 22.5°C (72.5°F) in all climates except for additional trials with 21°C (70°F) and 24°C (75°F) in the mixed climate of Knoxville, Tennessee. No thermostat setup or setback was modeled. Table 2 gives the seven pairs of solar reflectance and infrared emittance and Table 3 gives the values of roof thermal resistance that were used to include configurations of interest. For each entry, a brief description is given of the roof surface in Table 2 and of the roof construction in Table 3. For the eight locations selected, Table 4 gives the average daily solar irradiation of a horizontal surface, the cooling degree days, the heating degree days and additional data explained below.

TABLE 2.
Pairs of % Solar Reflectance (Rxx) and % Infrared Emittance (Eyy) Used in Development of an Estimating Tool for Selection of Cost Effective Low-Slope Roof Configurations

Code	Fully-Weathered Surface Condition
R70E90	High Reflectance White Latex Coating
R48E82	Low Reflectance White Latex Coating
R50E52	High Reflectance Aluminum Coating
R26E68	Low Reflectance Aluminum Coating
R33E90	Aluminized Asphalt Emulsion Coating
R64E11	Bare Aluminum Capsheet
R05E90	Uncoated Surface

TABLE 3.
Thermal Resistances Used in Development of an Estimating Tool for Selection of Cost Effective Low-Slope Roof Configurations

Code	R-value, $m^2 \cdot K/W$ ($h \cdot ft^2 \cdot °F/Btu$)	Roof Configuration[3]
R-5	0.84 (4.75)	3.8 cm (1.5 in.)-thick wood fiberboard insulation on a 1.9 cm (0.75 in.)-thick plywood deck
R-13	2.2 (12.6)	5.1 cm (2.0 in.)-thick aged polyisocyanurate insulation on a 0.9 mm-thick (20 gauge) Type B metal deck
R-25	4.4 (25.2)	10.2 cm (4.0 in.)-thick aged polyisocyanurate insulation on a 0.9 mm-thick (20 gauge) Type B metal deck
R-32	5.5 (31.5)	12.7 cm (5.0 in.)-thick aged polyisocyanurate insulation on a 0.9 mm-thick (20 gauge) Type B metal deck

[3]All roofs have built-up roof membranes or single-ply roof membranes that are assumed to add negligible thermal resistance. Cover boards or other fire retardants are also assumed to add negligible thermal resistance.

TABLE 4.
Locations Used in Development of an Estimating Tool for
Selection of Cost Effective Low-Slope Roof Configurations

Location	Average Daily Solar (Btu/h·ft²)	CDD_{65}[4]	HDD_{65}[5]	Cooling Index	Heating Index
Phoenix, Arizona	76.6	3814	1154	0.583	0.115
Miami, Florida	64.9	4126	141	0.536	0.014
Tampa, Florida	64.8	3311	697	0.429	0.070
Dallas, Texas	65.0	2414	2304	0.314	0.230
Knoxville, Tennessee	55.6	1366	3662	0.152	0.366
Boulder, Colorado	61.1	622	6012	0.076	0.601
Minneapolis, Minnesota	52.4	634	8002	0.066	0.800
Anchorage, Alaska	32.2	2	10395	0.0001	1.040

[4] Annual sum÷24 of hourly differences between hourly air temperature and 65°F when hourly air temperature is more than 65°F.
[5] Annual sum÷24 of hourly differences between 65°F and hourly air temperature when hourly air temperature is less than 65°F.

The challenge undertaken in this paper, and implemented at the Internet location http://www.ornl.gov/roofs+walls/facts/RadiationControl.htm, is to use the loads to produce an estimating tool. Its purpose is to assist owners and/or operators of buildings with low-slope roofs in selection of a radiation control configuration that is most cost effective for their situation. The estimating tool needs to be comprehensive and flexible. It cannot be overly complicated to use. Calculations with it cannot be too time-consuming to make estimates on an interactive web site. Therefore, equations in the form of polynomials were selected as the means to predict annual cooling and heating loads as a function of location, surface radiation properties (solar reflectance and infrared emittance) and roof insulation level (R-value). The effect of thermally massive decks is outside the scope of the estimating tool. See Wilkes et al. (2000) for a brief discussion of the effect of concrete decks on heating and cooling loads predicted by STAR.

Cooling loads and heating loads were treated separately. The influence of solar insolation was more evident in the cooling loads as a function of location than it was in the heating loads. A dimensionless and normalized cooling index, CI, was devised that went roughly from 0 to 1 for the range of locations in Table 4. The cooling index was the product of hourly average solar insolation and cooling degree days divided by 500,000. A dimensionless and normalized heating index, HI, was devised that went roughly from 0 to 1 for the range of locations in Table 4. The heating index was heating degree days divided by 10,000. The values 500,000 in CI and 10,000 in HI are the maxima of the respective numerators for the units listed in Table 4. Inspection of the cooling loads and heating loads showed that 60,000 Btu/ft² per year was the upper limit for the range of

locations. Therefore, coefficients were sought to give dimensionless and normalized cooling loads in the following form:

$$\frac{CL}{60000} = Ac \bullet CI + Bc \bullet CI^2 + Cc \bullet CI^3 \qquad (1)$$

where,

CL is the cooling load in Btu/ft² per year,
CI is the cooling index: (average hourly solar insolation)•CDD_{65}/500000, and
Ac, Bc and Cc are constants to fit the data.

Similarly, coefficients were sought to give dimensionless and normalized heating loads in the following form:

$$\frac{HL}{60000} = Ah \bullet HI + Bh \bullet HI^2 + Ch \bullet HI^3 \qquad (2)$$

where,

HL is the heating load in Btu/ft² per year,
HI is the heating index: HDD_{65}/10000, and
Ah, Bh and Ch are constants to fit the data.

Note that the form of Equations (1) and (2) satisfies the constraint that loads go to zero as the index goes to zero.

Regressions and exact fits were done to generate values for the coefficients of the polynominals in Equations (1) and (2). To generate the data to fit, these steps were taken:

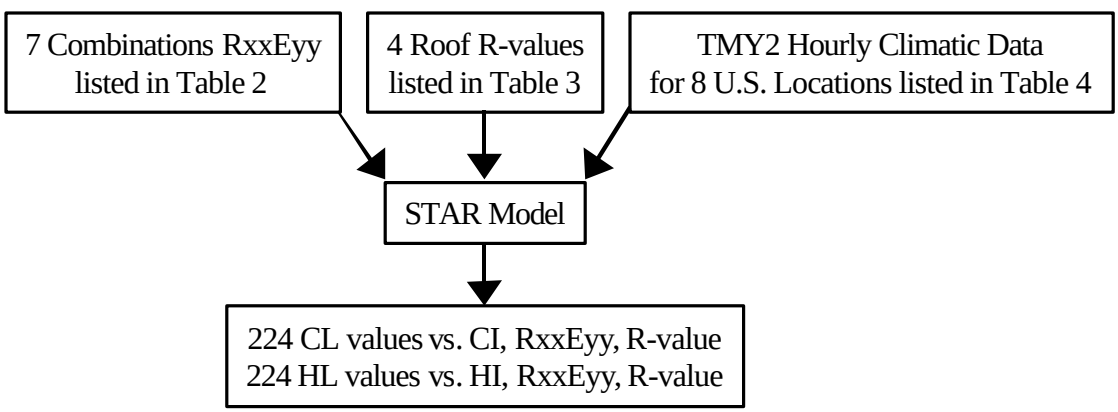

Then, for each of the seven RxxEyy pairs and each of the four R-values,

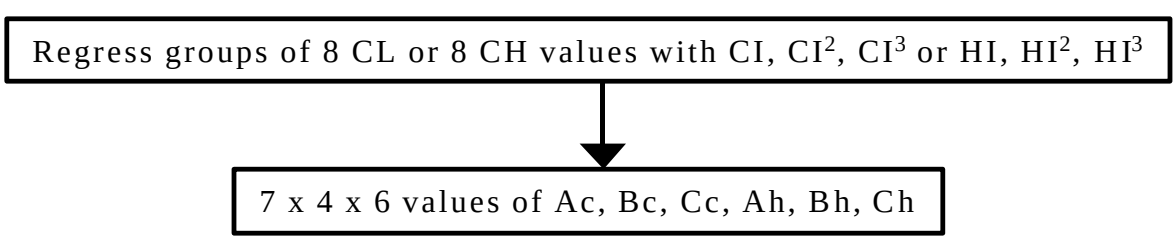

The coefficients of regression, r^2, for CL varied from 0.961 to 0.989. For HL, r^2 varied from 0.987 to 0.997. To capture the dependence on solar reflectance, infrared emittance and thermal resistance, let K_i = Ac, Bc, Cc, Ah, Bh or Ch and define

$$K_i = a_i + b_i \cdot \rho_{solar} + c_i \cdot \rho_{solar}^2 + d_i \cdot \epsilon_{infrared} \tag{3}$$

where,

ρ_{solar} is the solar reflectance, which varies from 5% to 70%,
$\epsilon_{infrared}$ is the infrared emittance, which varies from 11% to 90%, and
a_i, b_i, c_i and d_i are constants corresponding to each K_i.

Then, for each K_i = Ac, Bc, Cc, Ah, Bh or Ch,

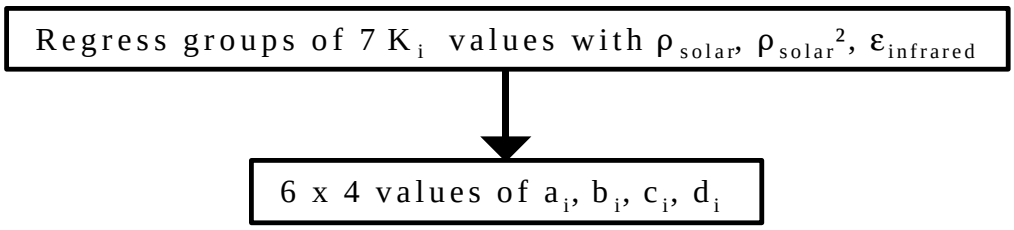

The form of Equation (3) was used successfully to correlate annual averages of measurements such as membrane temperature with thermal radiation properties in the RCMA project. The appropriateness for use to develop the estimating tool is indicated by the coefficients of regression, r^2, for the various a_i, b_i, c_i and d_i in Equation (3). They were all greater than 0.998. This is not surprising because the data were generated by a model.

Finally, for each K_i = Ac, Bc, Cc, Ah, Bh or Ch, the four values of a_i, b_i, c_i or d_i for thermal resistances of R-5, R-13, R-25 and R-32, respectively, were fit exactly to equations of the form:

$$a_i = a1_i + a2_i \bullet R + a3_i \bullet R^2 + a4_i \bullet R^3 \tag{4a}$$
$$b_i = b1_i + b2_i \bullet R + b3_i \bullet R^2 + b4_i \bullet R^3 \tag{4b}$$
$$c_i = c1_i + c2_i \bullet R + c3_i \bullet R^2 + c4_i \bullet R^3 \tag{4c}$$
$$d_i = d1_i + d2_i \bullet R + d3_i \bullet R^2 + d4_i \bullet R^3 \tag{4d}$$

where,

R is the thermal resistance of the roof,
$a1_i$, $a2_i$, $a3_i$ and $a4_i$ are the coefficients required to fit each a_i exactly with R,
$b1_i$, $b2_i$, $b3_i$ and $b4_i$ are the coefficients required to fit each b_i exactly with R,
$c1_i$, $c2_i$, $c3_i$ and $c4_i$ are the coefficients required to fit each c_i exactly with R, and
$d1_i$, $d2_i$, $d3_i$ and $d4_i$ are the coefficients required to fit each d_i exactly with R.

Exact fit of a third order polynomial was better than regression with a second order polynomial. Cooling and heating loads with the second order polynomial reached a minimum between R-25 and R-32. Thereafter the loads increased as R-value increased, which is not realistic. The 16 x 6 values for the constants, once generated and arranged in an array, allow very efficient prediction of a cooling load or a heating load for a particular location, solar reflectance, infrared emittance and roof thermal resistance.

Figure 4 is a worst case example of how well the estimating tool is able to predict the cooling loads generated by STAR. The highest insulation level of R-32 is selected as the worst case because cooling loads are relatively small. The symbols depict cooling

loads that STAR generated at R-32 for the seven RxxEyy combinations and eight locations. The curves from Equation (1) go smoothly through the corresponding STAR results. Labels are added to identify the location and their placement can be verified in Table 4. A third order polynomial does not fit exactly the complicated dependence of cooling load on location, especially for Tampa, Miami and Phoenix and also for Boulder and Minneapolis. The coefficients of regression from 0.961 to 0.989 show that the fit is good.

Figure 5 is a worst case example of how well the estimating tool is able to predict the heating loads generated by STAR. Again, the highest insulation level of R-32 is selected as the worst case because heating loads are relatively small. Data for Phoenix, Dallas, Knoxville and Boulder do not lie smoothly on the line calculated by Equation (2) but scatter is not as severe as it is in Figure 4. The coefficients of regression from 0.989 to 0.997 show that a third order polynomial is an excellent choice to fit the heating loads generated by STAR.

NET ANNUAL COST SAVINGS DUE TO RADIATION CONTROL

The estimating tool makes annual cooling and heating loads available for any location, solar reflectance, infrared emittance and roof thermal resistance of interest for a low-slope roof with a light weight deck. Cooling energy cost savings can be calculated for a proposed roof with solar radiation control relative to one without solar radiation control by the formula:

$$\$\text{cool} = \frac{\text{Ecool} \bullet \$\text{elec}}{\text{EFFcool}} \tag{5}$$

where,

$cool is annual cooling cost savings per unit area of roof,

Ecool is annual cooling energy savings in units of electricity use per unit area of roof,

$elec is average unit cost of electricity over the cooling season, and

EFFcool is seasonal cooling equipment efficiency.

Similarly, the heating energy cost savings can be calculated for a proposed roof with solar radiation control relative to one without solar radiation control by the formula:

$$\$\text{heat} = \frac{\text{Eheat} \bullet \$\text{fuel}}{\text{EFFheat}} \tag{6}$$

where,

$heat is annual heating cost savings per unit area of roof,

Eheat is annual heating energy savings in units of fuel use per unit area of roof,

$fuel is average unit cost of heating fuel over the heating season, and

EFFheat is seasonal heating equipment efficiency.

If $heat is negative, the heating penalty partially offsets the cooling savings. Annual operating cost savings are the sum of the cooling cost savings and the heating cost savings.

Note that the estimating tool produces the difference in annual energy costs for a roof with radiation control and one without radiation control for the user’s choice of

parameters. If the existing roof already has some radiation control, first it will need to be compared to one without radiation control. A roof with more radiation control can then be compared to one without radiation control. Manually taking the difference in savings between these cases will compare more radiation control to an existing level of radiation control.

Because the estimating tool always compares roofs with and without radiation control, the estimation is not restricted to the thermostat set point of 22.5°C (72.5°F) that was used in its development. Trials for Knoxville, Tennessee climatic data showed about the same linear behavior of heating and cooling loads with set points from 21°C (70°F) to 24°C (75°F) from no radiation control to the highest level of radiation control. Although cooling and heating loads with and without radiation control are sensitive to the set point, their differences are not. The implicit assumption is that the inside air temperature must be the same with and without radiation control. Estimates with the tool should be valid despite different thermostat set points during the heating and cooling seasons, as long as the same schedule is followed with and without radiation control. If, in practice, radiation control permits a higher cooling thermostat set point, the estimating tool will underpredict savings.

In Figures 6, 7 and 8, net cooling and heating operating cost savings are compared for two situations: the roof only with the estimating tool and a two-story, all-electric, office building with 560 m² (6,000 ft²) of low-slope roof. The annual operating energy savings for the office building were estimated using DOE2.1E (LBNL 1993) with a special function included in the input file. With this function, the deck heat fluxes from STAR for the roofs in the estimating tool were substituted in DOE2.1E for its roof deck heat fluxes before weighting factors were applied.

The U.S. Energy Information Administration maintains an internally searchable Internet website at http://www.eia.doe.gov/ with up-to-date statistical information about electricity and fuel costs for all U.S. energy production and consumption sectors. Average commercial electricity price for 1999 was $0.0723/KWh. Average natural gas price for the commercial sector for 1998 was $0.548/Therm for 1998 (EIA 2001). These data were used in preparation of Figures 6, 7 and 8.

The annual average coefficient of performance of the electric air-conditioning in the roof-only estimating tool was set at 3.0 while the average efficiency of the natural gas furnace was set at 0.90. These high values were chosen to yield conservative savings with the estimating tool. For the office building in DOE 2.1E, the electric air-conditioning had a design coefficient of performance of 2.9 and electric resistance heat was used with an efficiency of 1.00. Default part-load performance curves built into DOE2.1E were used for off-design operation of the equipment in the office building.

Operation of the office building in DOE2.1E included thermostat setback during heating and thermostat setup during cooling. The office building thermostat was at 22°C (72°F) for heating and at 24°C (76°F) for cooling from 07:00 to 18:00 weekdays. Otherwise it was at 16°C (60°F) for heating and 29°C (84°F) for cooling.

Annual electricity consumptions for the office building were obtained from the building energy performance summary produced by DOE2.1E for each RxxEyy on the abscissas in Figures 6, 7 and 8. Appropriate comparisons with a R05E90 roof were run separately. For each case, differences were formed to obtain energy savings. They were multiplied by the cost per unit of electricity to produce annual operating cost savings.

Finally, the annual operating cost savings were divided by total roof area to yield savings in $/ft² like were obtained directly from the estimating tool by Equations (5) and (6). For savings in $/m², multiply $/ft² by 10.76.

Figure 6 for Miami reinforces our previous conclusion (Wilkes et al. 2000) that white latex-coated surfaces R70E90 and R48E82 show the most savings relative to uncoated surfaces in cooling-dominated climates for poorly insulated roofs. Figure 7 for Knoxville and Figure 8 for Minneapolis reinforce the conclusion that the aluminum capsheet R64E11 shows the most savings in mixed and heating-dominated climates. Of most interest for this paper, however, are the relative sizes of savings using the estimator for the roof only compared to using DOE2.1E for the office building. For cases where the estimator predicts savings greater than about $0.02/ft² per year, the savings from the estimator are the same or slightly larger than those for the office building.

The relative effects of different surfaces and different amounts of thermal insulation are generally the same using the estimator and using DOE2.1E. The exceptions are the savings with the highest reflectance white latex coating R70E90 compared to those with the aluminum capsheet R64E11 in the mixed climate of Knoxville. The estimator predicts the capsheet is best; DOE2.1E predicts the white coating is slightly better for the office building.

The estimating tool was exercised for the roof of the office building using electric resistance heat at an efficiency of 1.00 instead of a natural gas furnace with an efficiency of 0.90. Electricity cost was taken to be the same for heating and for cooling. The very expensive electric heat ($2.12 per Therm with no heat pump benefit) made no difference in the comparison for Miami because there was so little heat required. In the mixed climate of Knoxville and the heating dominated climate of Minneapolis, electric heat exaggerated the heating penalty for radiation control, making savings for the surfaces R70E90 and R48E82 economically unattractive. The savings for the surface R64E11, on the other hand, more than doubled because of its low infrared emittance. Savings for the surface R50E52 remained about the same.

In buildings with high internal loads or high solar gain through windows, cooling may be needed and radiation control may be beneficial at times when the estimating tool predicts a heating penalty. The heating penalty is further exaggerated with electric resistance heat in the estimator because no thermostat setback is included in it. In the estimator, unlike in DOE 2.1E, heating load is assumed to directly affect the heating energy requirement regardless of when it occurs. A tool as simple as the estimator must be used with caution in complicated situations.

Comparisons between results with the estimating tool and DOE2.1E were made for a one-story, electric air-conditioned and natural-gas-heated warehouse with 3600 m² (38,600 ft²) of low-slope roof. In the same location, cooling costs per unit area of roof for the warehouse were about one-tenth of the values for the office building, implying that DOE2.1E was less sensitive to changes in radiation control on the roof of the warehouse. In Miami for the warehouse, DOE2.1E showed only about 20 to 25% of the savings predicted by the estimator in Figure 6. Savings (or losses) with radiation control from the DOE2.1E modeling of the warehouse varied from +$0.015 to -$0.015 per ft² (+$0.16 to -$0.16 per m²) in Knoxville and Minneapolis.

Early work by Griggs et al. (1989) with DOE2.1B used an office building, a retail store and an industrial warehouse as examples. Table 5 shows comparisons of net savings

in annual energy costs per unit area of a coated low-slope roof for the examples of Griggs et al. and the estimating tool. This early work assumed a constant infrared emittance of 0.9 for all surfaces. The industrial warehouse example was modified to low activity and low internal loads instead of the energy intensive designation of Griggs et al. Their energy intensive designation eliminates the heating penalty for a building in any climate, which yields more savings ($0.041/ft² or $0.44/m² in Minneapolis) than seems realistic. The few cases in Table 5 reinforce the conclusion from Figures 6, 7 and 8 that the estimator yields savings that are the same or slightly greater than savings from DOE2.1.

TABLE 5.
Comparison of Net Savings in Annual Energy Costs per Unit Area of a Coated Low-Slope Roof for the Examples of Griggs, et al.(1989) and the Estimating Tool for $\epsilon_{IR} = 0.9$

Case 1: Office Building; Albuquerque, NM; 5000 ft² R-4 Roof to $\rho_{solar} = 0.7$ from $\rho_{solar} = 0.2$; Cooling $0.109/KWh @ COP=1.7; Heating $0.47/Therm @ efficiency=0.75	
Annual Savings: Griggs, et al.	Annual Savings: Estimating Tool
$0.129/ft² ($1.39/m²)	$0.139/ft² ($1.50/m²)
Case 2: Retail Building; Dallas, TX; 10000 ft² R-9.2 Roof to $\rho_{solar} = 0.65$ from $\rho_{solar} = 0.05$; Cooling $0.099/KWh @ COP=1.7; Heating $0.54/Therm @ efficiency=0.75	
Annual Savings: Griggs, et al.	Annual Savings: Estimating Tool
$0.118/ft² ($1.27/m²)	$0.126/ft² ($1.36/m²)
Case 3: Industrial Building; Minneapolis, MN; 7000 ft² R-8 Roof to $\rho_{solar} = 0.65$ from $\rho_{solar} = 0.05$; Cooling $0.068/KWh @ COP=1.7; Heating $0.61/Therm @ efficiency=0.75	
Annual Savings: Griggs, et al.	Annual Savings: Estimating Tool
$0.016/ft² ($0.17/m²)	$0.015/ft² ($0.16/m²)

A significant feature of the estimator relative to DOE2.1E is the ease with which comparisons can be made for new situations. The left half of Table 6 illustrates this point by showing data using the estimator at conditions different from those in Figures 6, 7 and 8. Average commercial electricity price for 2000 was $0.0745/KWh and average natural gas price for the commercial sector was $0.533/Therm for 1999 (EIA 2001), about the same as the earlier values used for Figures 6, 7 and 8. Average coefficient of performance of the electric air conditioning is taken to be 2.5 not 3.0. Average heating efficiency is taken to be 0.85 not 0.90. These values are more realistic maxima. The decreases in efficiency are the main reason for increases in savings relative to the results in Figures 6, 7 and 8.

The right half of Table 6 shows the result of using another feature of the estimator. This feature addresses use of conventional insulation instead of radiation control. The values in the right half of Table 6 show how much conventional insulation would need to be present in a roof without radiation control for it to have the same annual operating cost as a roof with radiation control and the existing amount of insulation.

Adding conventional insulation to an existing roof may be more difficult than adding radiation control.

TABLE 6.
Net Savings in Annual Energy Costs per Square Foot of a Coated Low-Slope Roof and R-value for an Uncoated Roof with Same Annual Energy Costs as the Coated Low-Slope Roof [6]

	Net Savings ($/ft²) vs. R05E90			$R_{uncoated}$ for Net Savings = 0		
Miami	R70E90	R50E52	R64E11	R70E90	R50E52	R64E11
R-5 h·ft²·°F/Btu	$0.166	$0.077	$0.074	R-13	R-8	R-8
R-13 h·ft²·°F/Btu	$0.070	$0.032	$0.029	R-32	R-17	R-16
R-25 h·ft²·°F/Btu	$0.038	$0.017	$0.016	R-35	R-32	R-32
R-32 h·ft²·°F/Btu	$0.030	$0.013	$0.012	R-36	R-34	R-34
Knoxville	R70E90	R50E52	R64E11	R70E90	R50E52	R64E11
R-5 h·ft²·°F/Btu	$0.067	$0.047	$0.062	R-7	R-7	R-7
R-13 h·ft²·°F/Btu	$0.028	$0.018	$0.024	R-16	R-15	R-16
R-25 h·ft²·°F/Btu	$0.016	$0.010	$0.013	R-32	R-31	R-32
R-32 h·ft²·°F/Btu	$0.012	$0.008	$0.010	R-34	R-34	R-34
Minneapolis	R70E90	R50E52	R64E11	R70E90	R50E52	R64E11
R-5 h·ft²·°F/Btu	$0.015	$0.022	$0.037	R-5	R-6	R-6
R-13 h·ft²·°F/Btu	$0.006	$0.008	$0.013	R-14	R-14	R-14
R-25 h·ft²·°F/Btu	$0.004	$0.004	$0.007	R-25	R-28	R-29
R-32 h·ft²·°F/Btu	$0.002	$0.003	$0.005	R-32	R-33	R-33

[6] Uses $0.0745/KWh of electricity (year 2000 average) with air conditioner COP=2.5 and $0.533/Therm of natural gas (year 1999 average) with furnace efficiency=0.85.

Some of the conventional insulation R-values in the right half of Table 6 go slightly beyond the range of values used to develop the estimator. The equations yield reasonable results up to R-40 although economic interest in radiation control is limited at such high levels of conventional insulation. Early in the RCMA project before the test surfaces weathered, solar reflectances as high as 0.85 were observed. The equations in the estimating tool are well-behaved in solar reflectance to this level. Predictions of heating loads with them agreed within 5% with STAR-generated heating loads for $\rho_{solar} = 0.85$ and Knoxville, Tennessee climatic data over the range of R-values. Predictions of cooling load agreed within 2%. The equations are linear in infrared emittance so slight extrapolation beyond the range used in their development is allowable. The following ranges are considered valid for use of the estimator for all locations in the TMY2 data set: 0.9 m²·K/W (5 h·ft²·°F/Btu) < R-value < 7 m²·K/W (40 h·ft²·°F/Btu); 5% < ρ_{solar} < 85%; and, 5% < $\epsilon_{infrared}$ < 95%.

The current version of the estimating tool does not address the economic benefits of peak demand reduction due to radiation control on a building's low-slope roof. If the building's utility rates include large demand charges for electricity used during peak hours, radiation control may contribute to reduction in the demand charges. An estimating tool different from the one described in this paper would be needed to address this issue. Work on a tool to estimate peak reduction due to radiation control on low-slope roofs is in progress.

To illustrate some early results, recall that hourly deck heat fluxes were generated by the low-slope roof model STAR and were used to estimate annual heating and cooling loads. The deck heat fluxes for Miami, Florida and Knoxville, Tennessee were searched for the maximum deck heat flux that occurred during the cooling season. Table 7 shows the results for eight surfaces including a new, white latex-coated surface R85E90 (with solar reflectance of 85%). The last row of the table shows data for an uncoated, black surface R05E90. For each surface and the two locations, peak heat fluxes into the conditioned space and time of occurrence of the peak are listed. The deck heat fluxes in Table 7 for Knoxville are 10% to 25% larger than the peak insulation heat fluxes on the day selected for Figure 3 for surfaces R48E82, R26E68 and R05E90 (average of R05E87 and R05E92). Predictions for Figure 3 used measured climatic data for August 17, 1999.

TABLE 7.
Peak Deck Heat Fluxes from STAR with TMY2 Data for Miami and Knoxville and Estimate of Peak Power Reduction due to Radiation Control for an R-5 h·ft²·°F/Btu Roof

	Miami			Knoxville		
Surface	Peak Deck Heat Flux, Btu/(h·ft²)	Time of Peak	Power Reduction[7], W/ft²	Peak Deck Heat Flux, Btu/(h·ft²)	Time of Peak	Power Reduction[7], W/ft²
R85E90	5.8	6/26 14:00	1.56	5.3	6/20 16:00	1.70
R70E90	8.8	6/26 14:00	1.27	8.9	6/20 15:00	1.37
R48E82	13.8	8/16 14:00	0.78	14.3	6/28 14:00	0.82
R64E11	15.8	5/5 14:00	0.58	17.6	6/28 15:00	0.50
R50E52	15.4	8/16 14:00	0.63	16.6	6/28 14:00	0.60
R33E90	16.3	8/16 14:00	0.53	16.9	6/28 14:00	0.56
R26E68	19.6	5/5 14:00	0.21	20.7	6/28 14:00	0.19
R05E90	21.8	5/7 14:00	N.A.	22.7	6/28 14:00	N.A.

[7] Difference between peak deck heat fluxes for surfaces R05E90 and RxxEyy converted to electrical power used by cooling equipment assuming COP = 3.0. Not applicable for surface R05E90.

The differences between the peak heat flux for the uncoated surface and those for the other surfaces were taken, converted to W/ft² and divided by 3.0. The results are shown in the last column for each location. They are an estimate of electrical power reduction for cooling equipment per unit area of low-slope roof. The divisor 3.0 is a

reasonable coefficient of performance for modern cooling equipment at peak conditions. Total roof area and local demand charge per peak kW of demand are needed to determine cost savings.

The peak deck heat fluxes for the various surfaces in Miami occur at times that differ by three months. They occur in mid-August for surfaces R48E82, R50E52 and R33E90. Peaks in mid-August for surfaces R85E90 and R64E11 are 5% less than the listed values. Peaks in mid-August for surfaces R70E90, R26E68 and R05E90 are the same as the listed values. The peak deck heat fluxes for Knoxville all occur in late June. Variation in the peak deck heat fluxes does not appear to be large from month to month during the cooling season for each surface at each location.

The peak deck heat fluxes have about the same value for a particular surface in the two locations. The estimates of electrical power reduction due to the roof are also about the same for a particular surface in the two locations. Much work remains to be done to produce an estimating tool to predict the effect of a low-slope roof on monthly summer and winter peak demand for electricity. These preliminary results offer the hope that a simple but useful tool can be produced.

CONCLUSIONS

A solar radiation control fact sheet has been developed for low-slope roofs and appears at the Internet location http://www.ornl.gov/roofs+walls/facts/RadiationControl.htm. It features a simple interactive tool to estimate annual operating cost savings with radiation control due to total annual savings in energy use for cooling and heating. Alternately, it yields the amount of conventional insulation without radiation control that a roof needs in order to have the same annual energy costs as the roof with the existing amount of conventional insulation and solar radiation control. It does not address savings in peak demand due to radiation control.

Annual cooling and heating loads for low-slope roofs were obtained in previous work as a function of roof location, solar reflectance, infrared emittance and thermal insulation level. They were generated by a one-dimensional, transient heat transfer model validated by experiments at one location with one roof configuration and the commercially available range of solar reflectances and infrared emittances. This paper has shown that the polynomials used in the estimating tool reproduce well the variation in these loads due to changes in roof location, solar reflectance, infrared emittance and thermal insulation level.

Estimations with the interactive tool of annual operating cost savings per unit roof area were compared to operating cost savings from annual energy use predictions for whole buildings divided by their respective roof areas. The estimating tool for the roof only gave savings that were the same or slightly larger than several whole building results. The estimating tool generally showed the same dependence on changes in solar reflectance, infrared emittance and insulation level at three locations. The locations were characterized by a cooling-dominated climate, a mixed climate and a heating-dominated climate. The heating penalty due to radiation control may dominate results with the estimating tool in mixed and heating-dominated climates if expensive heating methods such as electric resistance heat are used.

REFERENCES

Akbari, H. and S. Konopacki. 1998. The impact of reflectivity and emissivity of roofs on building cooling and heating energy use. Proceedings, Thermal Performance of the Exterior Envelopes of Buildings VII, pp. 29-39. Atlanta, GA: American Society of Heating, Refrigerating and Air Conditioning Engineers.

Bretz, S.E. and H. Akbari. 1997. Long-term performance of high-albedo roof coatings. Energy and Buildings, Vol. 25, pp. 159-167.

Byerley, A.R. and J.E. Christian. 1994. The long term thermal performance of radiation control coatings. Proceedings 1994 ACEEE Summer Study on Energy Efficiency in Buildings, pp. 5.59-5.71. Washington, DC: American Council for an Energy Efficient Economy.

Childs, P.W., T.W. Petrie, and J.A. Atchley. 2001. Comparison of techniques for in situ, non-damaging measurement of infrared emittances of low-slope roof membranes. Submitted for review and publication in proceedings, Thermal Performance of the Exterior Envelopes of Whole Buildings VIII Conference, December 2-6, 2001, Clearwater Beach, Florida.

EIA. 2001. Form EIA-826, Monthly electric utility sales and Form EIA-176, Annual report of natural and supplemental gas supply and disposition. Internally search for EIA-826 and EIA-176 on Internet web site http://www.eia.doe.gov/. Washington, DC: U.S. Energy Information Admin.

Griggs, E.I., T.R.Sharp, and J.M. MacDonald. 1989. Guide for estimating differences in building heating and cooling energy due to changes in solar reflectance of a low-sloped roof. Report ORNL-6527. Oak Ridge, TN: Oak Ridge National Laboratory.

LBNL. 1993. DOE-2 supplement, version 2.1E. Report LBL-34947. Berkeley, CA: Lawrence Berkeley National Laboratory.

NREL. 1995. TMY2s. Typical meteorological years derived from the 1961-1990 national solar radiation data base. Data Compact Disk. Golden, CO: National Renewable Energy Laboratory.

Petrie, T.W., P.W. Childs, and J.E. Christian. 1998. Radiation control coatings on rough-surfaced roofs at a federal facility: Two summers of monitoring plus roof and whole building modeling. Proceedings, Thermal Performance of the Exterior Envelopes of Buildings VII, pp. 353-371. Atlanta, GA: American Society of Heating, Refrigerating and Air Conditioning Engineers.

Wilkes, K.E. 1989. Model for roof thermal performance. Report ORNL/CON-274. Oak Ridge, TN: Oak Ridge National Laboratory.

Wilkes, K.E., T.W. Petrie, J.A. Atchley, and P.W. Childs. 2000. Roof heating and cooling loads in various climates for the range of solar reflectances and infrared emittances observed for weathered coatings. Proceedings 2000 ACEEE Summer Study on Energy Efficiency in Buildings, pp. 3.361-3.372. Washington, DC: American Council for an Energy Efficient Economy.

LIST OF FIGURES

Fig. 1 Three-year history of solar reflectances for 26 low-slope roofs with effect of cleaning after three years.

Fig. 2 Comparison of measured and predicted membrane temperatures for two white latex-coated surfaces, four aluminum-coated surfaces and two uncoated surfaces on an R-5 $h \cdot ft^2 \cdot °F/Btu$ roof.

Fig. 3 Comparison of measured and predicted insulation heat fluxes for two white latex-coated surfaces, four aluminum-coated surfaces and two uncoated surfaces on an R-5 $h \cdot ft^2 \cdot °F/Btu$ roof.

Fig. 4 Example comparison of cooling loads generated by STAR to cooling loads calculated by the estimating tool with the procedure of Equations (1) through (4).

Fig. 5 Example comparison of heating loads generated by STAR to heating loads calculated by the estimating tool with the procedure of Equations (1) through (4).

Fig. 6 Comparison of annual operating cost savings per unit area of low-slope roof in Miami, Florida using the estimating tool and DOE2.1E for an office building.

Fig. 7 Comparison of annual operating cost savings per unit area of low-slope roof in Knoxville, Tennessee using the estimating tool and DOE2.1E for an office building.

Fig. 8 Comparison of annual operating cost savings per unit area of low-slope roof in Minneapolis, Minnesota using the estimating tool and DOE2.1E for an office building.

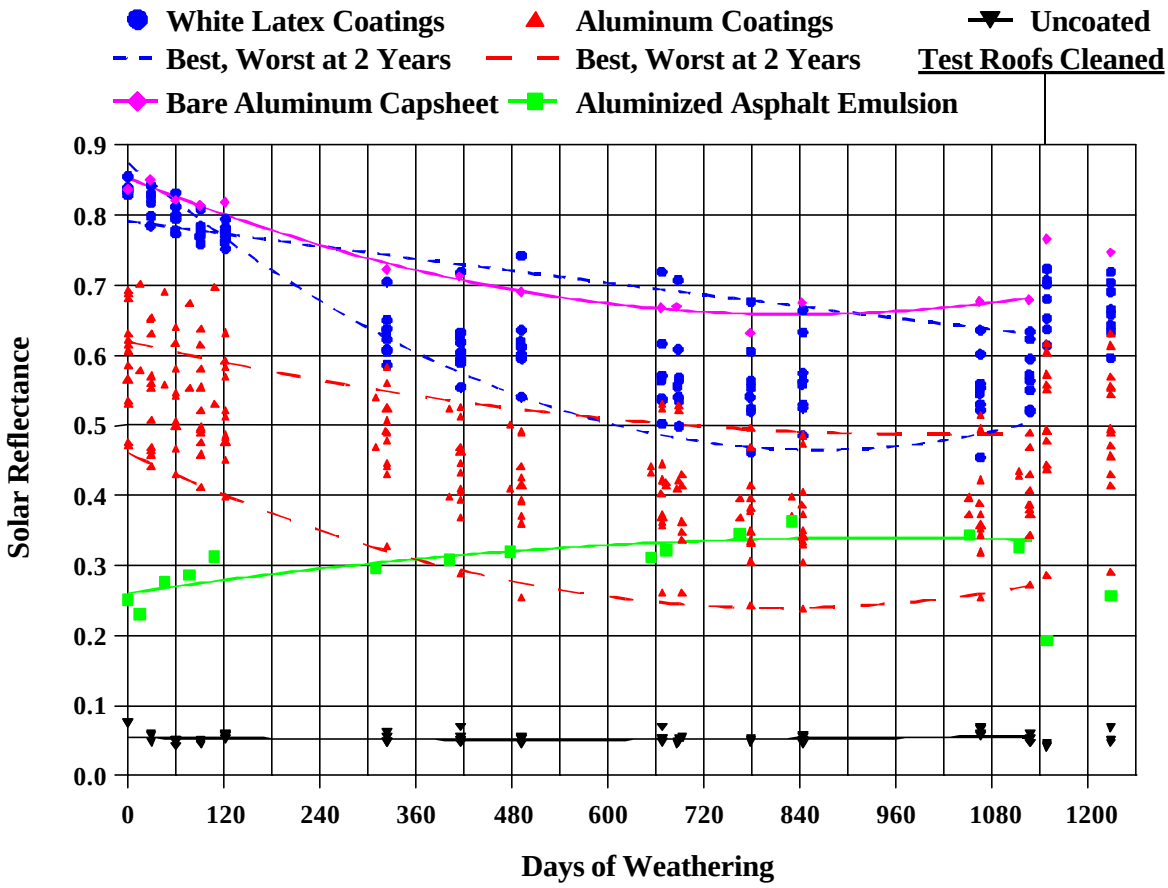
White Latex Coatings
Aluminum Coatings
Uncoated
Best, Worst at 2 Years
Best, Worst at 2 Years
Test Roofs Cleaned
Bare Aluminum Capsheet
Aluminized Asphalt Emulsion
Solar Reflectance
0.9
0.8
0.7
0.6
0.5
0.4
0.3
0.2
0.1
0.0
0
120
240
360
480
600
720
840
960
1080
1200
Days of Weathering

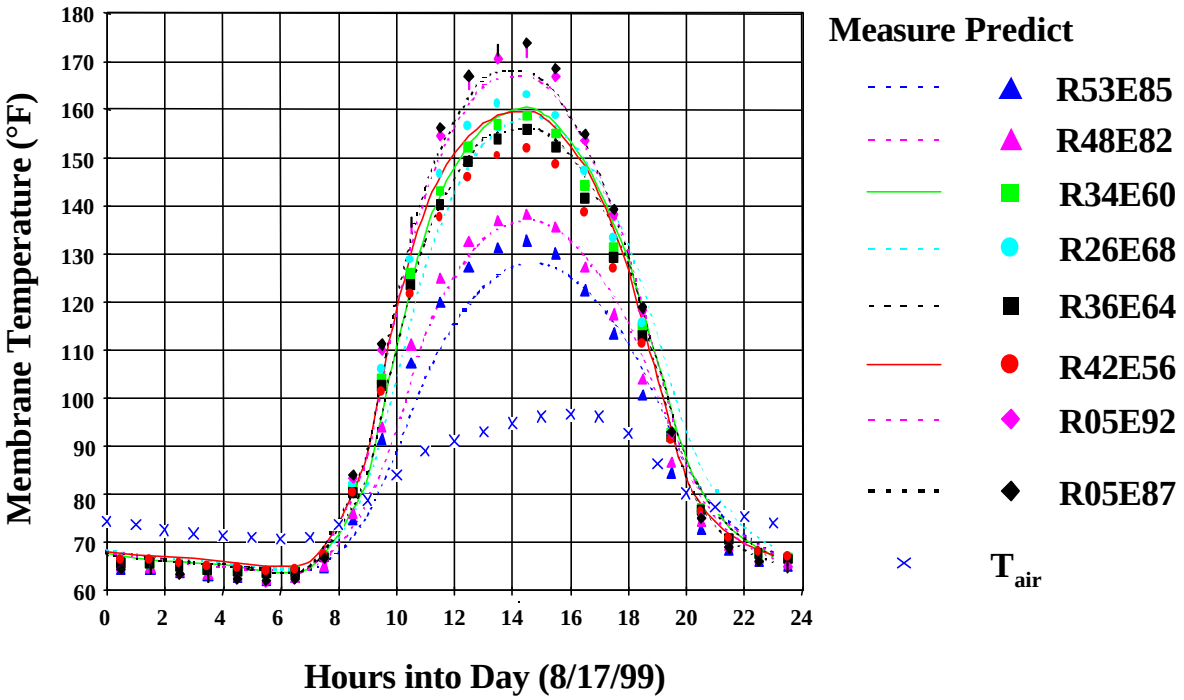
Membrane Temperature (°F)
180
170
160
150
140
130
120
110
100
90
80
70
60
0
2
4
6
8
10
12
14
16
18
20
22
24
Hours into Day (8/17/99)
Measure Predict
R53E85
R48E82
R34E60
R26E68
R36E64
R42E56
R05E92
R05E87
T air

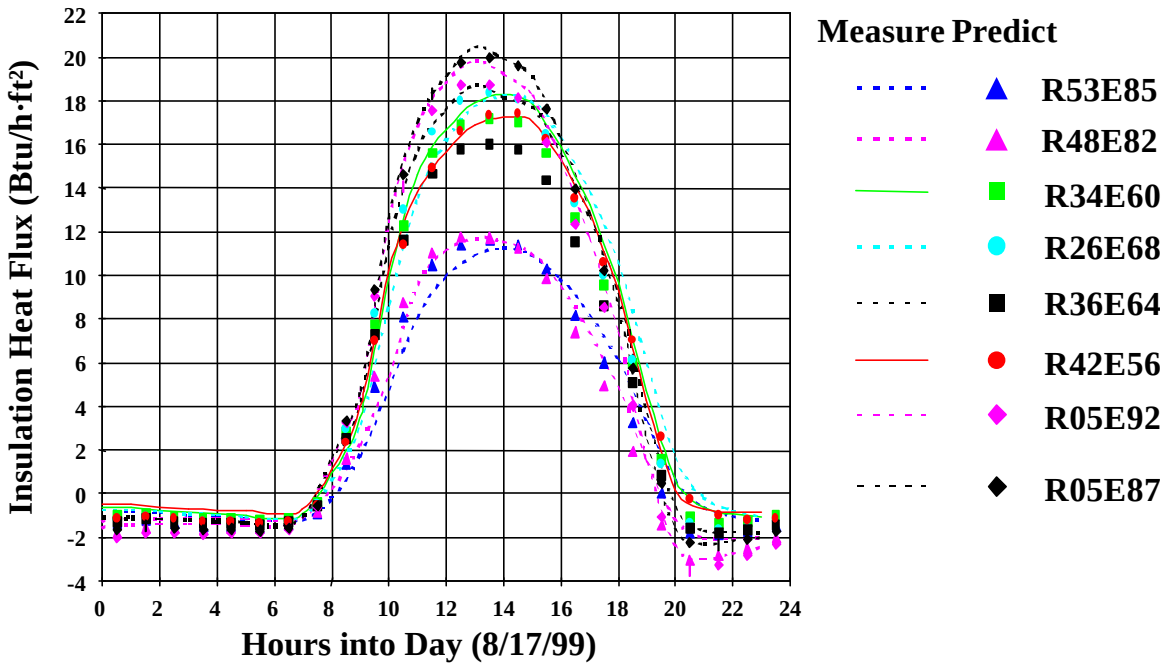
Insulation Heat Flux (Btu/h·ft²)
22
20
18
16
14
12
10
8
6
4
2
0
-2
-4
0
2
4
6
8
10
12
14
16
18
20
22
24
Hours into Day (8/17/99)
Measure Predict
R53E85
R48E82
R34E60
R26E68
R36E64
R42E56
R05E92
R05E87

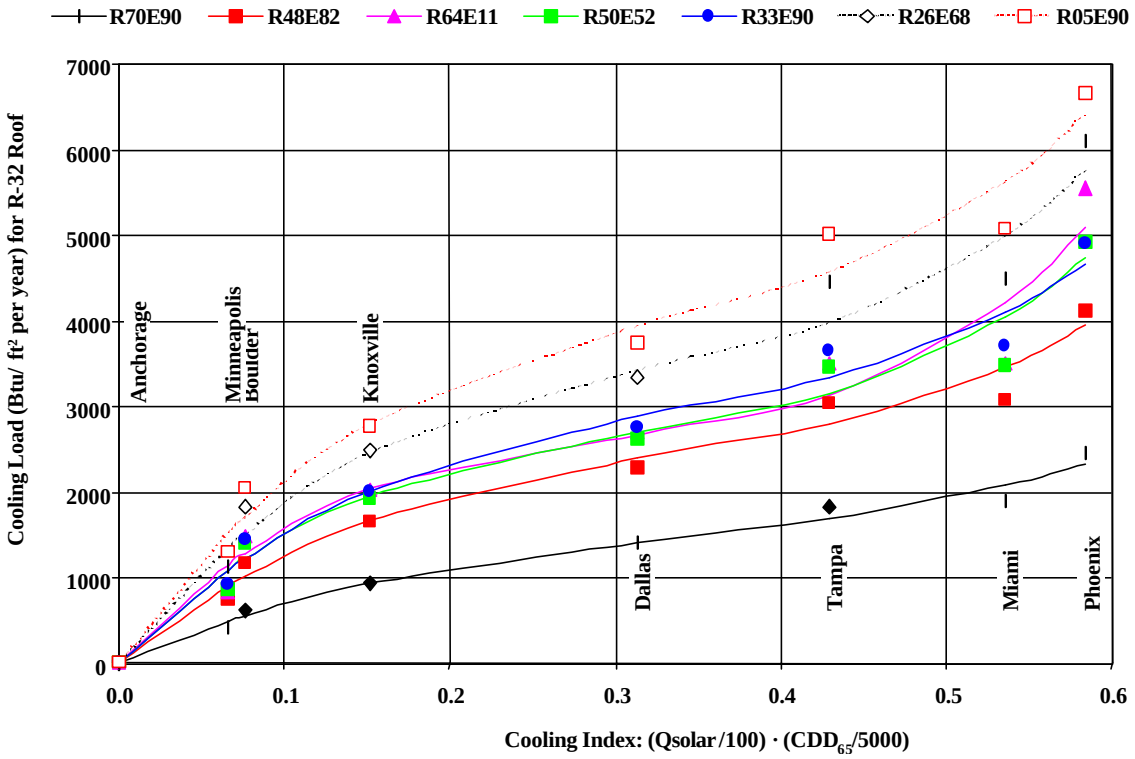
R70E90
R48E82
R64E11
R50E52
R33E90
R26E68
R05E90
Cooling Load (Btu/ ft² per year) for R-32 Roof
7000
6000
5000
4000
3000
2000
1000
0
0.0
0.1
0.2
0.3
0.4
0.5
0.6
Cooling Index: (Qsolar/100) · (CDD65/5000)
Anchorage
Minneapolis
Boulder
Knoxville
Dallas
Tampa
Miami
Phoenix

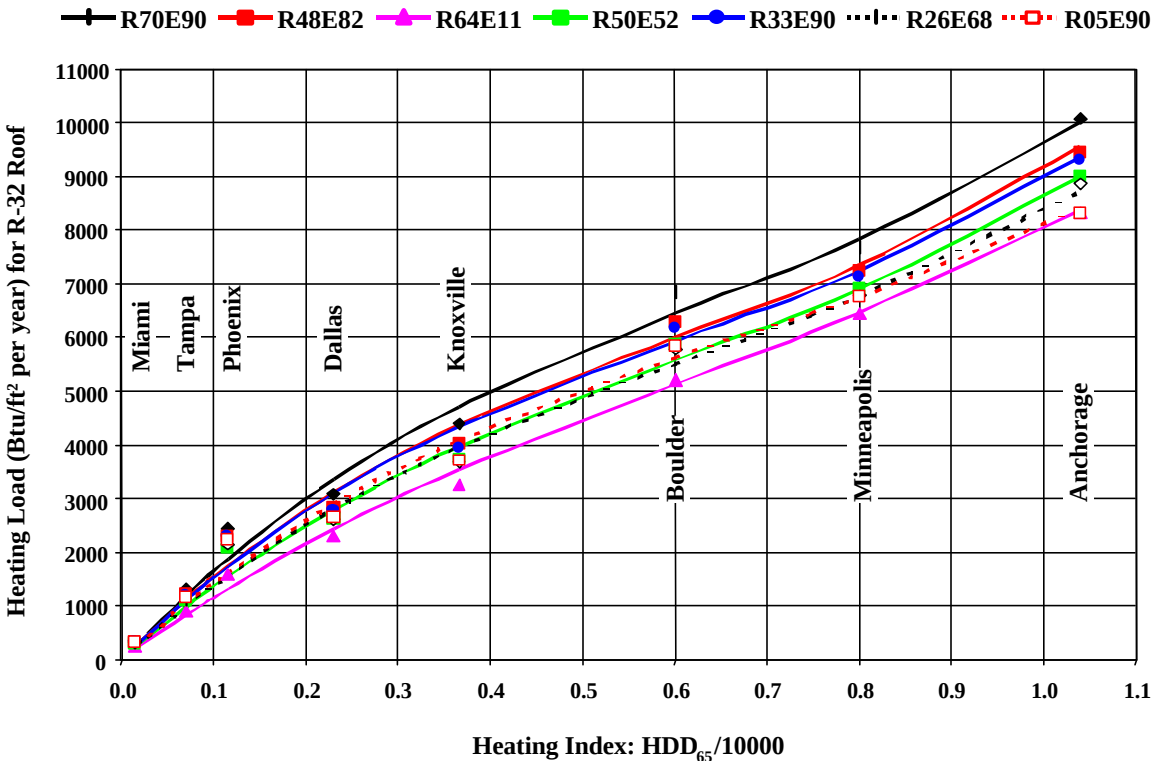
R70E90
R48E82
R64E11
R50E52
R33E90
R26E68
R05E90
Heating Load (Btu/ft² per year) for R-32 Roof
11000
10000
9000
8000
7000
6000
5000
4000
3000
2000
1000
0
Miami
Tampa
Phoenix
Dallas
Knoxville
Boulder
Minneapolis
Anchorage
0.0
0.1
0.2
0.3
0.4
0.5
0.6
0.7
0.8
0.9
1.0
1.1
Heating Index: HDD65/10000

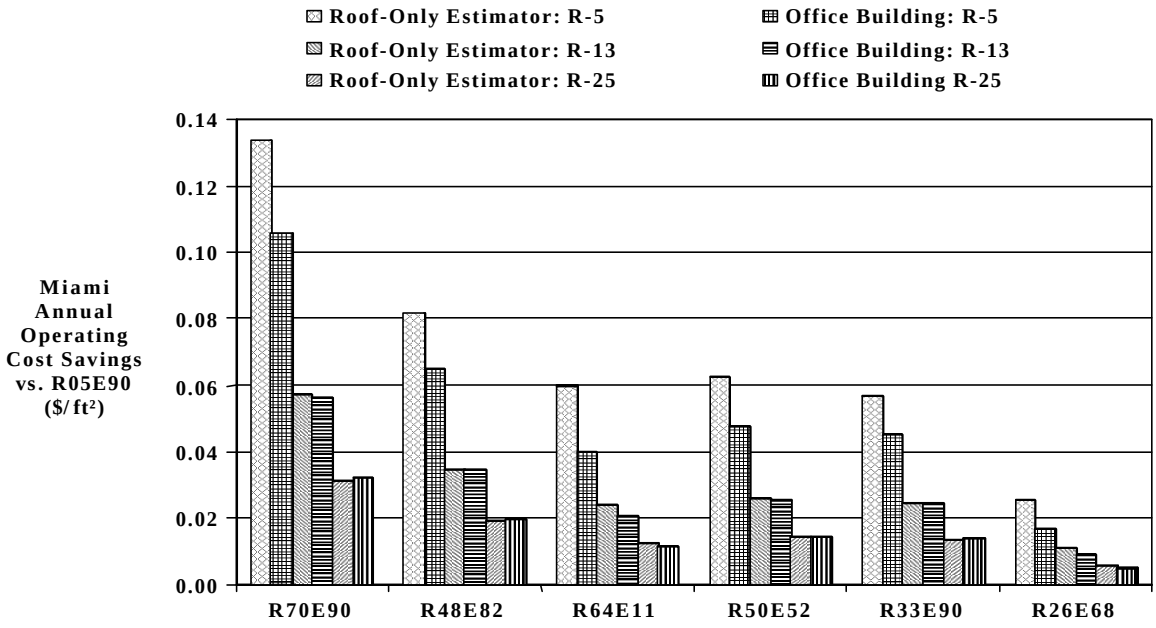
Roof-Only Estimator: R-5
Roof-Only Estimator: R-13
Roof-Only Estimator: R-25
Office Building: R-5
Office Building: R-13
Office Building R-25
Miami Annual Operating Cost Savings vs. R05E90 ($/ft²)
0.14
0.12
0.10
0.08
0.06
0.04
0.02
0.00
R70E90
R48E82
R64E11
R50E52
R33E90
R26E68

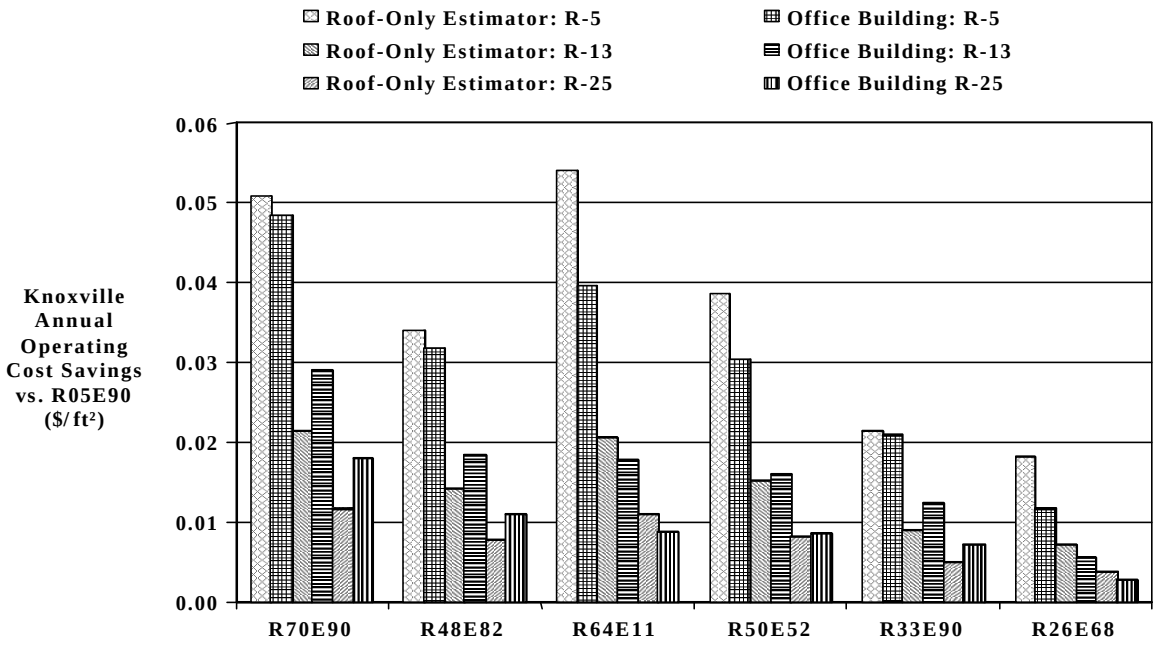
Roof-Only Estimator: R-5
Roof-Only Estimator: R-13
Roof-Only Estimator: R-25
Office Building: R-5
Office Building: R-13
Office Building R-25
Knoxville Annual Operating Cost Savings vs. R05E90 ($/ft²)
0.06
0.05
0.04
0.03
0.02
0.01
0.00
R70E90
R48E82
R64E11
R50E52
R33E90
R26E68

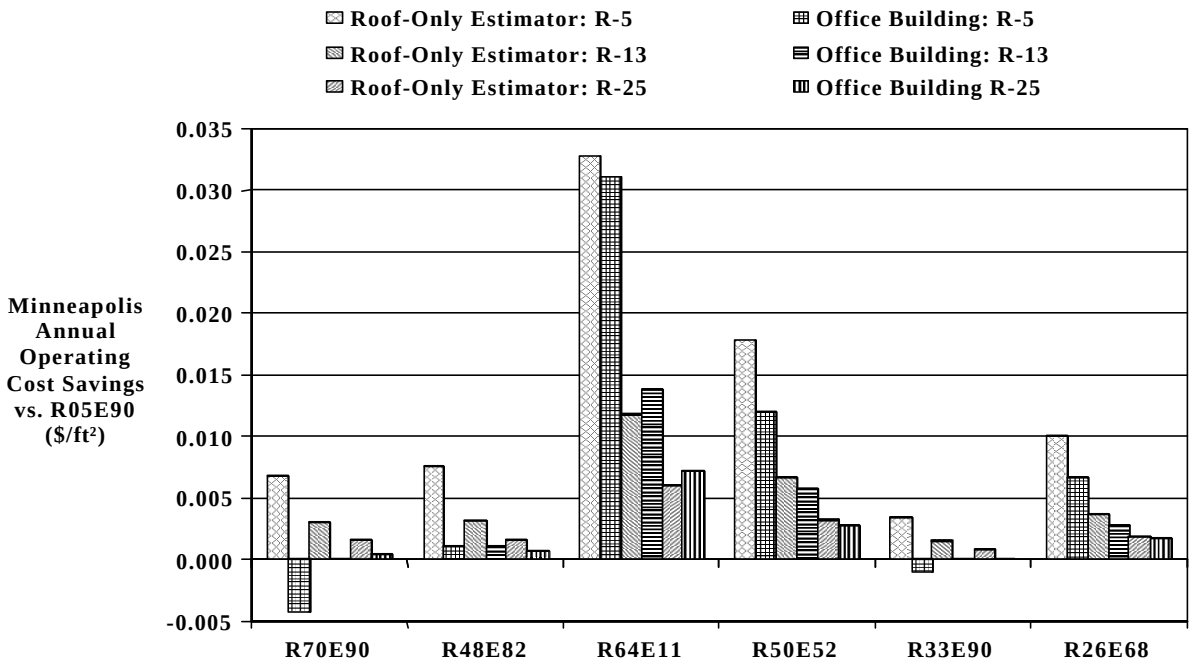
Roof-Only Estimator: R-5
Roof-Only Estimator: R-13
Roof-Only Estimator: R-25
Office Building: R-5
Office Building: R-13
Office Building R-25
Minneapolis Annual Operating Cost Savings vs. R05E90 ($/ft²)
0.035
0.030
0.025
0.020
0.015
0.010
0.005
0.000
-0.005
R70E90
R48E82
R64E11
R50E52
R33E90
R26E68